Elasticity of sphere packings: pressure and initial state dependence

I. Agnolin & J.-N. Roux
Laboratoire des Matériaux et des Structures du Génie Civil, Institut Navier, Champs-sur-Marne, France

arXiv:0901.2287v1 [cond-mat.mtrl-sci] 15 Jan 2009

ABSTRACT: Elastic properties and internal states of isotropic sphere packings are studied by numerical simulations. Several numerical protocols to assemble dense configurations are compared. One, which imitates experiments with lubricated contacts, produces well coordinated states, while another, mimicking the effect of vibrations, results, for the same density, in a much smaller coordination number z, as small as in much looser systems. Upon varying the confining pressure P, simulations show a very nearly reversible variation of density, while z is irreversibly changed in a pressure cycle. Elastic moduli are shown to be mainly related to the coordination number. Their P dependence notably departs from predictions of simple homogenization approaches in the case of the shear moduli of poorly coordinated systems.

1 INTRODUCTION

The mechanical properties of solidlike granular materials are well known to depend on the internal structure of the packing. Classically, one distinguishes between the behaviour of dense and loose materials (Wood 1990; Mitchell 1993). However, some results – see e.g. (Benahmed et al. 2004) – also indicate that other factors than the sole packing fraction (or void index) also determine the quasistatic response to applied load variations. In numerical simulations, it is a common practice to remove friction in the assembling stage in order to prepare dense samples (Makse et al. 1999; Thornton 2000). It is not guaranteed that the correct initial state, as obtained in laboratory experiments, is reproduced. Elastic properties, or sound wave velocities, are now commonly measured in soil mechanics (Chen et al. 1988; Hicher 1996) and condensed matter physics (Jia et al. 1999) laboratories. Their evaluation in numerical calculations can allow for comparisons with experiments.

We report here on a numerical study of isotropically assembled and compressed sphere packings, prepared in different initial states. Coordination numbers are found to vary according to the preparation method independently from density, and to determine the elastic moduli and their pressure dependence.

2 MODEL AND NUMERICAL METHODS

Numerical samples of 4000 identical balls of diameter a and mass m are prepared by standard molecular dynamics calculations, involving periodic boundary conditions in all three directions. The method is similar to those of Cundall & Strack (1979) or Thornton (2000), except that stresses, rather than strains, are controlled, as in (Parrinello & Rahman 1981). Contact elasticity relates the normal force F_N is to the normal deflection h of the contact by the Hertz law

$$F_N = \frac{\tilde{E}\sqrt{a}}{3}h^{3/2}, \text{ with } \tilde{E} = \frac{E}{1-\nu^2}, \qquad (1)$$

while variations of tangential elastic forces $\mathbf{F}_T$ with tangential displacements $\delta\mathbf{u}_T$,

$$\frac{d\mathbf{F}_T}{d\delta\mathbf{u}_T} = \alpha_T\frac{dF_N}{dh}, \text{ with } \alpha_T = \frac{2(1-\nu)}{2-\nu}, \qquad (2)$$

are modeled with a simplified form of the Cattaneo-Mindlin-Deresiewicz theory (Johnson 1985). On implementing (2), special care was taken, as advocated by Elata & Berryman (1996), to avoid spurious creation of elastic energy.

Particles are endowed with the Young modulus $E = 70$ GPa and the Poisson coefficient $\nu = 0.3$ of glass beads. The tangential reaction is limited by the Coulomb condition with friction coefficient $\mu = 0.3$.

First, the sample is assembled from an initial disordered loose granular gas state, under the prescribed isotropic pressure $P = 10$ kPa. In procedure A, tangential forces are suppressed in this stage, as for frictionless grains. This produces dense samples with a coordination number z^*, counting only force-carrying grains and contacts, approaching 6 in the rigid limit (Roux 2000). Only a small fraction $f_0 \simeq 1.3\%$ of grains (the "rattlers") carry no force. This procedure, already used in other numerical work (Thornton 2000), amounts to dealing with

perfectly lubricated beads. Imperfect lubrication can be modelled with a very small friction coefficient, $\mu_0 = 0.02$, resulting in slightly different samples, denoted as B configurations.

A different assembling procedure (method C) was designed to simulate dense samples obtained by vibration. Configurations A are first dilated, scaling all coordinates by a common factor $\lambda = 1.005$, thereby supressing the contacts ; then the grains are attributed random velocities and mixed with a kinetic-energy preserving event-driven ("hard sphere") calculation, until each of them has undergone 50 collisions on average ; finally, they are compressed with strongly dissipative collisions and friction, to mechanical equilibrium under $P = 10$ kPa. Remarkably (see table 1), such configurations C are very nearly as dense as the perfectly lubricated ones A, and actually denser than B ones, while their active coordination number z^* is considerably lower, with many more rattlers.

Finally, procedure D consists in directly compressing the granular gas to equilibrium at 10 kPa with the final coefficient of friction $\mu = 0.3$. z^* values are close to the C case, but the density is significantly lower.

Table 1 summarizes the data on these initial states. All data throughout this paper are averaged over 5 different samples, error bars correspond to one r.m.s. deviation. These initial states are then further compressed, on applying pressure steps, up to 100 MPa, assuming contacts still behave elastically, and then the pressure is gradually decreased back to 10 kPa. To ensure quasistatic conditions are maintained with sufficient accuracy, strain rates $\dot{\epsilon}$ are constrained by condition $\dot{\epsilon}\sqrt{\frac{m}{aP}} < 10^{-4}$. Equilibrium states are recorded for pressure values at ratio $\sqrt{10}$. Throughout this process, the friction coefficient is maintained equal to 0.3, for all four configuration types. Elastic constants are measured on building the stiffness matrix associated with the contact network at equilibrium.

Table 1. Packing fraction Φ, coordination number z^* on force-carrying structure and proportion of rattlers f_0 at the lowest pressure 10 kPa for the four simulated preparation procedures.

State	Φ	z^*	f_0 (%)
A	0.637 ± 0.009	6.074 ± 0.002	1.3 ± 0.2
B	$0.627 \pm 2 \cdot 10^{-4}$	5.80 ± 0.007	1.65 ± 0.02
C	0.635 ± 0.002	4.56 ± 0.03	13.3 ± 0.5
D	0.606 ± 0.002	4.62 ± 0.01	10.4 ± 0.9

3 RESULTS

3.1 *Structure of equilibrium configurations*

The results obtained on samples A, C and D are reported below, configurations of type B behaving very similarly to A ones. Fig. 1 displays the evolution of packing fraction Φ and coordination number z^* over the compression-decompression cycle. Changes in Φ are very nearly reversible (elastic): density differences between states A, C and D, are maintained at low pressure after one cycle, although A and C samples exhibit very similar properties at high P. The shape

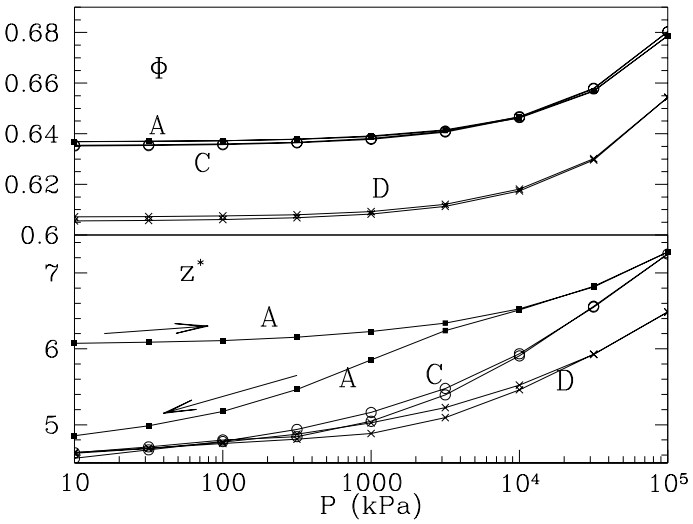

Figure 1. Variations of Φ and z^* as P increases up to 100 MPa and decreases back to 10 kPa, in samples A (square dots), C (open circles), and D (crosses).

of the normal force distribution also changes with P. It can be characterized by the reduced moments:

$$Z(\alpha) = \frac{\langle F_N^\alpha \rangle}{\langle F_N \rangle^\alpha}, \tag{3}$$

while the average normal force, for monosized beads, simply relates to P as

$$\langle F_N \rangle = \frac{\pi a^2 P}{z\Phi}, \tag{4}$$

$z = z^*(1 - f_0)$ being the total coordination number. The width of this distribution, as expressed, e.g., by $Z(2)$, decreases at growing P, the fastest in well-coordinated A samples. Changes in friction mobilization are also observed : as P grows, it first decreases in C and D samples, and increases in A ones (in which it starts at zero).

The change of z^* in type A samples as P decreases from a high value – many more contacts are lost than were gained at increasing P – might seem surprising. One should note however that configurations with a high coordination number, for nearly rigid grains, are extremely rare. Each contact requires a new equation to be satisfied by the set of sphere centre positions. Equilibrium states of rigid, frictionless sphere assemblies, apart from the motion of the scarce rattlers, are isolated points in configuration space, because of isostaticity (Roux 2000). As isotropic compression, at the microscopic scale, is not reversible, due to friction and to geometric changes, one should not expect exceptional configurations to be retrieved upon decreasing the pressure. Large coordination numbers of A (or B) samples do not survive a pressure cycle. The history of an isotropic sample can therefore significantly influence its structure without any appreciable density change.

3.2 *Elastic moduli*

Bulk (B) and shear (G) moduli of all equilibrium states for ascending P were computed on solving linear systems of equations involving the stiffness matrix (they express the response to infinitesimal stress changes). Their variations with P are plotted on Fig. 2. Results for configurations B (not shown) are very close to those of A samples. The obvious first

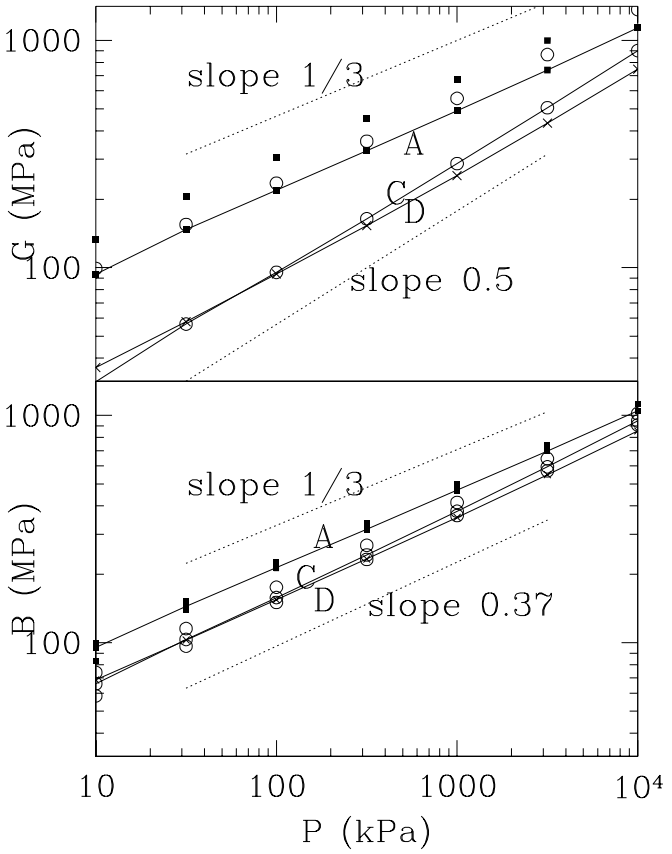

Figure 2. P dependence of bulk moduli B (bottom) and shear moduli G (top) (symbols for A, C, D states as on fig. 1, joined by continuous lines), and of their upper (B and G) and lower (for B only) bounds for states A and C (same symbols, no line). Note the relatively narrow bracketing of B in all cases, and the large overestimation of G by its Voigt upper bound in C samples.

conclusion to be drawn is that elastic moduli are sensitive to coordination rather than density, as results for states C and D are very similar. The pressure dependence of bulk moduli differs a little between A samples on the one hand and C, D on the other. In the latter case, the increases of B with P is slightly faster than the $P^{1/3}$ law predicted by simple estimates (see below). The most striking behaviour is that of G in samples C and D, the increase of which approaches a $P^{1/2}$ dependence. To explain such observations, one can try to estimate the moduli as follows. Assuming the distribution of normal forces is known, one gets by virtue of (1) and (2) the distribution of contact stiffnesses. It is easy, then, to derive upper bounds to B and G, and a lower bound to B, analogous to the Voigt and Reuss bounds for elastic heterogeneous continua (Nemat-Nasser & Hori 1993). The Voigt upper bound is the simple "effective medium" estimate that results from the assumption of affine displacement fields. Using the properties and notations introduced in Eqns. 1, 2, 3 and 4, one gets:

$$B \leq B^{\text{Voigt}} = \frac{1}{2}\left(\frac{z\Phi\tilde{E}}{3\pi}\right)^{2/3} P^{1/3} Z(1/3)$$
$$G \leq G^{\text{Voigt}} = \frac{6+9\alpha_T}{10} B^{\text{Voigt}}. \quad (5)$$

To write a lower bound (Reuss estimate), one needs a trial set of equilibrium contact force increments corresponding to the stress increment. For a simple increase of isotropic pressure, this is readily obtained by a scaling of the forces corresponding to the pre-existing pressure. Hence a lower bound for B (but no such estimate is available for G). Denoting as r_{TN} the ratio $||\mathbf{F}_T||/F_N$ in each contact, and defining

$$\tilde{Z}(5/3) = \frac{\langle F_N^{5/3}(1+\frac{r_{TN}^2}{\alpha_T})\rangle}{\langle F_N\rangle^{5/3}},$$

a modified reduced moment $Z(5/3)$ (Eqn. 3), one has:

$$B \geq B^{\text{Reuss}} = \frac{1}{2}\left(\frac{z\Phi\tilde{E}}{3\pi}\right)^{2/3} \frac{P^{1/3}}{\tilde{Z}(5/3)}. \quad (6)$$

In view of the force distribution and mobilization of friction observed, B, bracketed by (5) and 6, cannot depart very much from a $P^{1/3}$ dependence (r_{TN}^2/α_T is at most 0.11 anyway for $\mu=\nu=0.3$, and the product $Z(1/3)Z(5/3)$ only exceeds 1.15 for systems with few contacts at low pressure). As to the increase of z with P, it does not appear to entail large effects either.

The behaviour of G for samples C and D is quite different. G seems to get unexpectedly small ($G < B/2$) at low pressure. Its upper bound is a very poor estimate in such cases (as, by (5), $G^{\text{Voigt}} = 1.34 \times B^{\text{Voigt}}$). The situation is reminiscent of frictionless sphere packings (O'Hern et al. 2003), for which $G \ll B$ under isotropic pressure in the rigid limit. We could observe that those states had the largest level of strain fluctuations (departure from affine displacement field).

4 CONCLUSION

Our simulations of isotropically assembled sphere packings revealed the following points.

- Configurations of a given density can vary considerably in coordination number. Samples assembled with a procedure designed to imitate vibration can have a large density and a small coordination number.

- Elastic moduli are primarily sensitive to coordination numbers.

- They vary with pressure in rather good agreement to simple predictions (nearly as $P^{1/3}$, with a small effect of contact creation as P increases) in highly coordinated samples, but the shear modulus behaves quite anomalously in poorly coordinated ones, with a low value at low P and a faster increase, nearly as $P^{1/2}$ in some cases.

- A compression-decompression cycle, although almost reversible in terms of density, can substantially reduce the coordination number when it was initially high.

We therefore suggest to use elastic moduli, which can be compared between simulations and experiments, as indicators of the internal state (contact density) of granular packings.

On comparing numerically predicted ultrasonic wave velocities with experimental values obtained on dense sphere packs with P in the range 100-800 kPa, we observe (Agnolin et al. 2005) that perfectly lubricated samples (type A or B), are considerably too stiff, even though they agree with experimental observations in the MPa range (Makse et al. 1999). Although somewhat idealized, our "vibrated" ones (type C) seem to be closer to the materials studied in the laboratory. We also note in another contribution to the present proceedings (Roux 2005) that their stress-strain curves under growing deviatoric stress are also closer to experimentally observed mechanical behaviours. Of course, it will be necessary in the near future to investigate by numerical simulations more "realistic" assembling procedures (Emam et al. 2005), and the effects of the resulting anisotropy.

REFERENCES

Agnolin, I., Roux, J.-N., Massaad, P., Jia, X., & Mills, P. 2005. Sound wave velocities in dry and lubricated granular packings: numerical simulations and experiments. These proceedings.

Benahmed, N., Canou, J., & Dupla, J.-C. 2004. Structure initiale et liquéfaction statique d'un sable. *C.R. Académie des Sciences (Mécanique)* 332: 887–894.

Chen, Y.-C., Ishibashi, I., & Jenkins, J. T. 1988. Dynamic shear modulus and fabric: part I, depositional and induced anisotropy. *Géotechnique 38*(1): 23–32.

Cundall, P. A. & Strack, O. D. L. 1979. A discrete numerical model for granular assemblies. *Géotechnique 29*(1): 47–65.

Elata, D. & Berryman, J. G. 1996. Contact force-displacement laws and the mechanical behavior of random packs of identical spheres. *Mechanics of Materials* 24: 229–240.

Emam, S., Canou, J., Corfdir, A., Dupla, J.-C., & Roux, J.-N. 2005. Granular packings assembled by rain deposition: an experimental and numerical study. These proceedings.

Hicher, P.-Y. 1996. Elastic properties of soils. *ASCE Journal of Geotechnical Engineering* 122: 641–648.

Jia, X., Caroli, C., & Velicky, B. 1999. Ultrasound propagation in externally stressed granular media. *Phys. Rev. Lett.* 82: 1863–1866.

Johnson, K. L. 1985. *Contact Mechanics*. Cambridge University Press.

Makse, H., Gland, N., Johnson, D., & Schwartz, L. 1999. Why effective medium theory fails in granular materials. *Physical Review Letters 83*(24): 5070–5073.

Mitchell, J. K. 1993. *Fundamentals of soil behavior*. New York: Wiley.

Nemat-Nasser, S. & Hori, M. 1993. *Micromechanics: overall properties of heterogeneous materials*. North-Holland.

O'Hern, C., Silbert, L. E., Liu, A. J., & Nagel, S. R. 2003. Jamming at zero temperature and zero applied stress: The epitome of disorder. *Physical Review E 68*(1): 011306.

Parrinello, M. & Rahman, A. 1981. Polymorphic transitions in single cystals: A new molecular dynamics method. *Journal of Applied Physics* 52: 7182–7190.

Roux, J.-N. 2000. Geometric origin of mechanical properties of granular materials. *Physical Review E* 61: 6802–6836.

Roux, J.-N. 2005. The nature of quasistatic deformation in granular materials. These proceedings.

Thornton, C. 2000. Numerical simulations of deviatoric shear deformation of granular media. *Géotechnique* 50: 43–53.

Wood, D. M. 1990. *Soil Behaviour and Critical State Soil Mechanics*. Cambridge University Press.